

Weibull Effective Volumes and Surfaces for Cylindrical Rods Loaded in Flexure

George D. Quinn**

Ceramics Division, National Institute of Standards and Technology (NIST), Gaithersburg, Maryland 20899

Formulas are given for the effective volumes and effective surfaces for cylindrical rods that have been loaded in flexure. Strength scaling for specimen size usually is dependent on whether the flaws are volume- or surface-distributed. Flexural loadings of rods of constant diameter are an exception. The ratio of three-point flexural strengths to four-point flexural strengths is independent of whether the flaws are volume- or surface-distributed. Rods that have been tested in flexure do not expose much material to the maximum stresses. Large rods produce strengths that are comparable to common standardized rectangular bend bars for volume flaws. For surface flaws, smaller rectangular bar specimens actually have larger effective surfaces.

I. Introduction

WEIBULL effective volumes and surfaces are used to scale ceramic strengths from one component size to another, or from one loading configuration to another.¹ Larger specimens or components are likely to be weaker, because of the greater chance of them having a larger, more-severe flaw. The Weibull weakest-link model² leads to a strength dependency on component size:

$$\frac{\sigma_1}{\sigma_2} = \left(\frac{V_{E2}}{V_{E1}} \right)^{1/m} \quad (1)$$

where σ_1 and σ_2 are the mean (or median or characteristic) strengths of specimens of type 1 and 2 (which may have different sizes and stress distributions), V_{E1} and V_{E2} are the effective volumes, and m is the Weibull modulus. A unimodal flaw population that is uniformly distributed throughout the volume and a Weibull two-parameter distribution are assumed. Additional information on the Weibull model and its correlation to flaw-size distributions may be found in the work by Jayatilaka and Trustrum³ and Danzer.⁴

In the simplest case of direct uniform tension, V_E is assumed to be the specimen volume V . Many specimens or components such as flexural loaded rods or bars have stress gradients and $V_E < V$. Sometimes, the relationship between the two is expressed as $V_E = KV$, where K is the loading factor and V is the total volume within the outer loading points. V_E is the volume of a hypothetical tensile specimen, which, when subjected to the stress σ_{max} , has the same probability of fracture as the flexure specimen stressed at σ_{max} . In other words, a flexure bar of volume V is equivalent to a tensile specimen of size V_E .

If surface flaws predominate, then the strength scales with the effective surface areas (S_E):

$$\frac{\sigma_1}{\sigma_2} = \left(\frac{S_{E2}}{S_{E1}} \right)^{1/m} \quad (2)$$

Usually, the strength ratios predicted by Eqs. (1) and (2) differ. Fractographic analysis should be undertaken to determine the spatial distribution of the flaws. Even if fractographic analysis is not possible, strength ratios from actual data for two component configurations may be compared to the predicted ratios to infer whether the flaws were surface- or volume-distributed. An earlier work,⁵ which was a review of the flexural-strength test method, includes a list of cases wherein flexural-strength data correlated well with data from other test geometries or even components when scaled in accordance with Eqs. (1) or (2).

Tabulations of formulas for V_E or S_E for square or rectangular beam specimens loaded in flexure are readily available (see, for example, the work in Davies,¹ Weil and Daniel,⁶ or my companion paper⁷); however, formulas for cylindrical rods are more difficult to find or are incomplete.^{8–13} For illustrative purposes, effective volumes for two simple cases are derived below and then a complete tabulation is furnished. The formulas are applied to two problems: (i) scaling strengths of rods of constant diameter and (ii) a comparison of predictions of strength scaling to actual data from rods and rectangular bars for a silicon nitride.

II. Weibull Effective Volume

Figure 1 shows the flexural loading configurations. The effective volume, V_E , is given by

$$V_E = \int_V \left(\frac{\sigma_x}{\sigma_{max}} \right)^m dV \quad (\text{for } \sigma_x \geq 0) \quad (3)$$

where V is the total volume of the flexure specimen between the outer loading points, σ_x the uniaxial tensile stress along the x -axis, and σ_{max} the maximum outer fiber tensile stress. σ_{max} is the reference stress that is conventionally used for Weibull scaling for the purposes of comparison. The integration is performed over the portions of the specimen that are stressed in tension. The effective volume for a rod of radius R and length L_T for the case of uniform bending (Fig. 1(a)) along the beam length is

$$V_E = L_T \int_A \left(\frac{\sigma_x}{\sigma_{max}} \right)^m dA \quad (4)$$

where A is the rod cross-sectional area. Referring to Fig. 2, the stress varies linearly with distance from the neutral axis (r):

$$\sigma_x = \left(\frac{r}{R} \right) \sigma_{max} \quad (5a)$$

B. Cox—contributing editor

Manuscript No. 186942. Received May 29, 2002; approved October 7, 2002. Supported by the U.S. Department of Energy, Office of Transportation Technologies, Heavy Vehicle Propulsion Systems Materials Program (under Contract No. DE-AC05-84OR21400, with Martin Marietta Energy Systems, Inc.). **Fellow, American Ceramic Society.

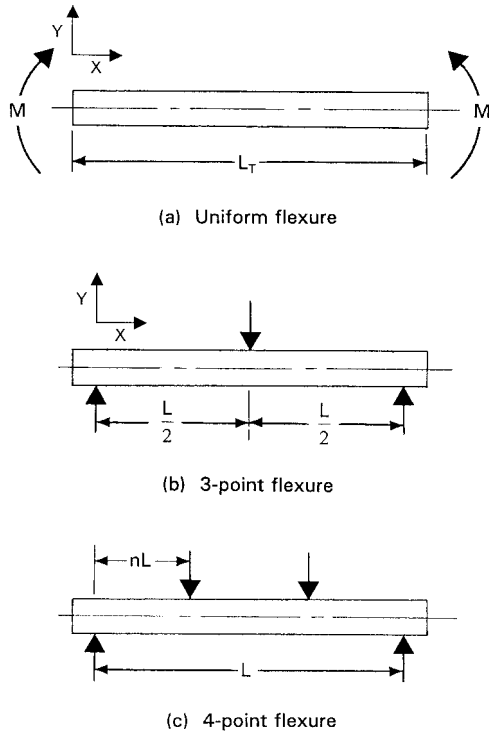


Fig. 1. Beam loading configurations.

and

$$dA = 2\ell dr \quad (5b)$$

and

$$\ell = [R^2 - r^2]^{1/2} \quad (5c)$$

$$dA = 2[R^2 - r^2]^{1/2} dr \quad (5d)$$

Then, combining Eqs. (4) and (5) yields

$$\begin{aligned} V_E &= L_T \int_A \left[\frac{(r/R)\sigma_{\max}}{\sigma_{\max}} \right]^m dA = L_T \int_0^R \left(\frac{r}{R} \right)^m (2[R^2 - r^2]^{1/2}) dr \\ &= \frac{2L_T}{R^m} \int_0^R r^m [R^2 - r^2]^{1/2} dr \end{aligned} \quad (6)$$

The solution for the definite integral, and using $V = L_T \pi R^2$, leads to

$$V_E = \left(\frac{2L_T}{R^m} \right) \left[\left(\frac{1}{2} \right) R^{m+2} \right] \left[\frac{\Gamma\left(\frac{m+1}{2}\right)\Gamma\left(\frac{3}{2}\right)}{\Gamma\left(\frac{m+4}{2}\right)} \right] = L_T R^2 G = \left(\frac{V}{\pi} \right) G \quad (7a)$$

where G is a combined gamma function:

$$G = \frac{\Gamma\left(\frac{m+1}{2}\right)\Gamma\left(\frac{3}{2}\right)}{\Gamma\left(\frac{m+4}{2}\right)} \quad (7b)$$

G is shown in Fig. 3 for the range of Weibull moduli that are typical of ceramic strength distributions. The effective volume for

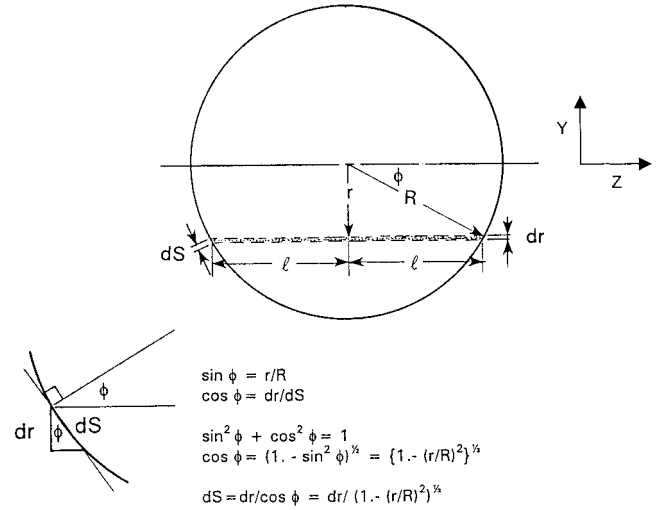


Fig. 2. Cylinder cross-section for the effective volume and surface analyses. For the effective volume, the material in the shaded zone $2l dr$ is integrated over the cross section. For the effective surface analysis, the surface length dS is integrated over the periphery. The insert shows details of the surface length geometry.

a three-point flexure specimen of length L between the outer spans (Fig. 1(b)) is given as

$$V_E = 2 \int_0^{L/2} \int_A \left(\frac{\sigma_x}{\sigma_{\max}} \right)^m dA dx \quad (8)$$

σ_x varies not only with r but also with position along the x -axis:

$$\sigma_x = \left(\frac{r}{R} \right) \left(\frac{2x}{L} \right) \sigma_{\max} \quad (9)$$

Then,

$$\begin{aligned} V_E &= 2 \int_0^{L/2} \int_A \left[\frac{\left(\frac{r}{R} \right) \left(\frac{2x}{L} \right) \sigma_{\max}}{\sigma_{\max}} \right]^m dA dx \\ &= \frac{2^{m+1}}{R^m L^m} \int_0^{L/2} \int_A r^m x^m dA dx \\ &= \frac{2^{m+1}}{R^m L^m} \int_0^{L/2} \int_0^R r^m x^m 2[R^2 - r^2]^{1/2} dr dx \\ &= \frac{2^{m+2}}{R^m L^m} \left(\frac{1}{m+1} \right) \left(\frac{L}{2} \right)^{m+1} \int_0^R r^m [R^2 - r^2]^{1/2} dr \\ &= \frac{2L}{(m+1)R^m} \left[\left(\frac{1}{2} \right) R^{m+2} \right] G \\ &= \left(\frac{LR^2}{m+1} \right) G = \left[\frac{V}{\pi(m+1)} \right] G \end{aligned} \quad (10)$$

Effective volumes for other configurations are listed in Table I.

III. Weibull Effective Surfaces

Effective surfaces may be similarly derived:

$$S_E = \int_S \left(\frac{\sigma_x}{\sigma_{\max}} \right)^m dA \quad (11)$$

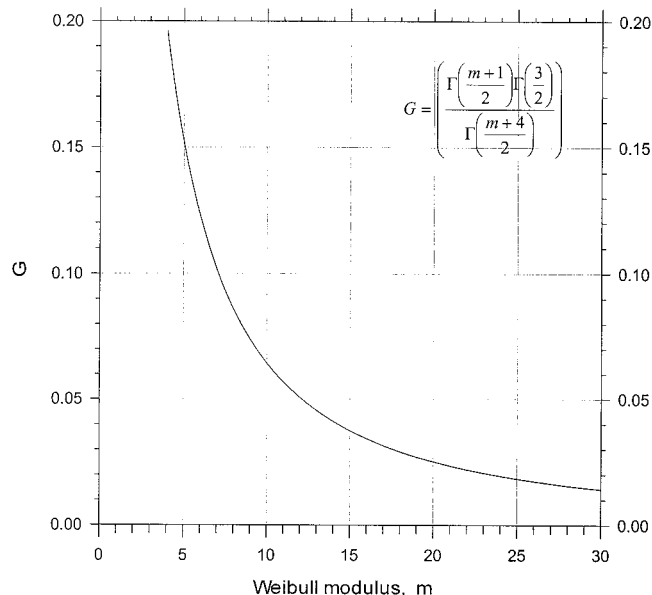


Fig. 3. G , the combined gamma function, as a function of Weibull modulus, m .

where the integration is performed over all tensile loaded surfaces. For a cylindrical rod of total length L_T in uniform bending (Fig. 1(a)) and referring to Fig. 2:

$$S_E = L_T \int_S \left(\frac{\sigma_x}{\sigma_{\max}} \right)^m dS = L_T \int_S \left[\frac{\left(\frac{r}{R} \right) \sigma_{\max}}{\sigma_{\max}} \right]^m dS \quad (12)$$

The insert in Fig. 2 shows

$$dS = \frac{dr}{[1 - (r/R)^2]^{1/2}} \quad (13)$$

Then,

$$S_E = 2L_T \int_0^R \left(\frac{r}{R} \right)^m \frac{dr}{[1 - (r/R)^2]^{1/2}} = \frac{2L_T}{R^m} \int_0^R r^m R(R^2 - r^2)^{-1/2} dr$$

$$= \frac{2L_T}{R^{m-1}} \int_0^R r^m (R^2 - r^2)^{-1/2} dr \quad (14)$$

The factor of 2 comes from the surface elements on both sides of the cross section. The definite integral in the last term on the right is similar to, but not exactly the same as, that for the effective volume problem. Substituting for the definite integral gives

$$S_E = \frac{2L_T}{R^{m-1}} \left[\frac{1}{2} (R^m) \right] \left[\frac{\Gamma\left(\frac{m+1}{2}\right)\Gamma\left(\frac{1}{2}\right)}{\Gamma\left(\frac{m+2}{2}\right)} \right] = L_T R G' \quad (15)$$

This combined gamma function G' is very similar to, but not exactly the same as, the combination G for effective volume. The two are related:

$$\Gamma(n+1) = n\Gamma(n) \quad (16a)$$

thus,

$$\Gamma\left(\frac{3}{2}\right) = \frac{1}{2} \left[\Gamma\left(\frac{1}{2}\right) \right] \quad (16b)$$

and

$$\Gamma\left(\frac{m+4}{2}\right) = \Gamma\left[\left(\frac{m+2}{2}\right) + 1\right] = \frac{m+2}{2} \left[\Gamma\left(\frac{m+2}{2}\right) \right] \quad (17)$$

such that

$$G' = \frac{\Gamma\left(\frac{m+1}{2}\right)\Gamma\left(\frac{1}{2}\right)}{\Gamma\left(\frac{m+2}{2}\right)} = \frac{\Gamma\left(\frac{m+1}{2}\right)2\Gamma\left(\frac{3}{2}\right)}{\left(\frac{m+2}{2}\right)\Gamma\left(\frac{m+4}{2}\right)}$$

$$= (m+2)G \quad (18)$$

The total area S between the outer loading points is $2\pi RL_T$; then, the effective surface for the uniformly stressed rod is given as

$$S_E = L_T R G' = L_T R (m+2)G = \frac{S}{2\pi} (m+2)G \quad (19)$$

The effective surfaces for other flexure configurations are given in Table I.

Earlier it was stated that strength scaling for size requires knowledge of whether flaws are volume- or surface-distributed. Although this is true for most general conversions, some flexural-strength conversions are curious exceptions. From Table I and Eq. (1), comparing three-point to four-point 1/4-point flexure strengths of *different length rods* of the same diameter ($2R$) gives

$$\frac{\sigma_{3pt}}{\sigma_{4pt}} = \left(\frac{V_{E,4pt}}{V_{E,3pt}} \right)^{1/m} = \left\{ \frac{\left[\frac{m+2}{2\pi(m+1)} \right] G \pi R^2 L_4}{\left[\frac{1}{\pi(m+1)} \right] G \pi R^2 L_3} \right\}^{1/m}$$

$$= \left(\frac{m+2}{2} \right)^{1/m} \left(\frac{L_4}{L_3} \right)^{1/m} \quad (20)$$

Also,

$$\frac{\sigma_{3pt}}{\sigma_{4pt}} = \left(\frac{S_{E,4pt}}{S_{E,3pt}} \right)^{1/m} = \left\{ \frac{\left[\frac{(m+2)^2}{4\pi(m+1)} \right] G 2\pi R L_4}{\left[\frac{m+2}{2\pi(m+1)} \right] G 2\pi R L_3} \right\}^{1/m}$$

$$= \left(\frac{m+2}{2} \right)^{1/m} \left(\frac{L_4}{L_3} \right)^{1/m} \quad (21)$$

The strength ratios are identical, irrespective of the fixture span lengths. Similarly, scaling strengths between any two rod flexural loadings can be shown to give the same volume and surface ratios, provided that the rod diameter is constant. This surprising coincidence of the strength ratios also applies to rectangular flexure specimens, provided that the beams have identical cross-sectional size.⁷

An illustrative example wherein rod strengths are compared to rectangular bar strengths is shown in Fig. 4, which shows data for a commercial sintered reaction-bonded silicon nitride (SRBSN) in which both specimen types broke from almost-identical machining crack flaws. Matching flexural-strength sets of rods and bars that have been prepared from the same material, with the same machining conditions, and that fracture from the same flaw types, are quite rare. These data were collected as part of a large study on the effects of machining on rod and bar strengths for this particular material.¹⁴ Preliminary results have been published previously.¹⁵ Hundreds of specimens were ground using a variety of procedures, fractured, and then fractographically examined. Data sets usually comprised thirty test specimens; however, in some instances, as few as ten specimens were tested, because of material availability or machining limitations. The strength distributions varied greatly depending on the machining conditions and the flaws that were

Table I. Effective Volumes and Surfaces for Flexural Loaded Cylinders[†]

Configuration	Effective volume, V_E	Effective surface, S_E
Uniform bending	$V(1/\pi)G$	$S[(m+2)/(2\pi)]G$
Three-point	$V(1/\pi)[1/(m+1)]G$	$S[(m+2)/(2\pi)][1/(m+1)]G$
Four-point, general [‡]	$V(1/\pi)\{1/[2(m+1)]\}[4n+2(m+1)(1-2n)]G$	$S[(m+2)/(2\pi)]\{1/[2(m+1)]\}[4n+2(m+1)(1-2n)]G$
Four-point, $1/4$ -point	$V(1/\pi)\{(m+2)/[2(m+1)]\}G$	$S[(m+2)/(2\pi)]\{(m+2)/[2(m+1)]\}G$
Four-point, $1/3$ -point	$V(1/\pi)\{(m+3)/[3(m+1)]\}G$	$S[(m+2)/(2\pi)]\{(m+3)/[3(m+1)]\}G$

[†]Note the similarities in the constants. The surface constants differ from the volume constants by $(m+2)/2$. V is the total volume between the outer loading points (πR^2L), and S is the total surface ($2\pi RL$). [‡]The inner loading points are located at a distance nL inward from either outer support point. For example, for four-point, $1/4$ -point loading, $n = 1/4$.

activated by the strength tests. Rods often had different strengths than comparably machined bars. The example shown in Fig. 4 is one of the few instances wherein the rods and bars were ground to the same specification and had almost-identical machining flaws. Thorough fractographic analysis on every specimen conclusively confirmed that the strength-limiting flaws were parallel machining cracks, 10–15 μm deep, in both the bars and the rods. Some of these flaws were linked with inherent material flaws, such as pores or agglomerates. Machining cracks are surface-distributed flaws by definition, according to ASTM Standard C 1322,¹⁶ and it was appropriate to apply Weibull area scaling to compare the strengths.

The rods were 6.0 mm in diameter and 110 mm long and were transversely ground with a 600 grit diamond wheel. The rods were tested on a four-point flexure fixture with 40- and 80-mm spans. The bars were four-point flexure specimens with dimensions of 3 mm \times 4 mm \times 50 mm, prepared in accordance with ASTM Standard C 1161, and were tested on 20- and 40-mm spans. The surface finish of the rods and bars were almost the same: $R_a = 0.140$ and $0.094 \mu\text{m}$, respectively. (R_a is average roughness.) Additional details on the material and the testing conditions are given in the work by Quinn *et al.*¹⁴

Figure 4 shows that the rods were slightly stronger than the bars. The Weibull parameters were estimated in accordance with ASTM Standard C 1239.¹⁷ The characteristic strengths (735 and 754 MPa) are not statistically significantly different, given the small

sampling size ($n = 10$).^{†,17,18} Nevertheless, it is instructive to compare rod and bar strengths by Weibull scaling for illustrative purposes. The bars actually had a larger effective surface than the rods: 85.0 mm² versus 58.8 mm², respectively. For this calculation, an average Weibull modulus of $m = 27.4$ was arbitrarily used; however, the conclusion is still valid for a wide range of m values. These are 15.2% and only 3.9% of the bar and rod total surfaces. Note the much-better surface efficiency of the rectangular bars. Equation (2) predicts that the bars should be 1.7% weaker than the rods, which is similar to the data that shows a 2.5% difference. Of course, the small sampling size ($n = 10$) causes significant uncertainty in these comparisons; however, m values from as low as 12 to as high as 36 do not change the simple conclusion that the bars have more effective surface than the rods do.

Although fractography conclusively proved that flaws were surface-distributed in this instance, it is instructive to compare the effective volumes. Although the rods were much larger than the bars, the Weibull effective volumes were similar: 6.00 mm³ and

[†]The Weibull parameters were estimated by a maximum likelihood analysis, in accordance with ASTM Standard C 1239. The 90% confidence bounds on the Weibull modulus estimates are 19.9–48.6 and 10.4–25.6 for the bars and rods, respectively. The bounds for the characteristic strengths are 723–747 MPa and 732–777 MPa, respectively. Confidence bound factors may be obtained from Tables 2 and 3 in ASTM Standard C 1239, which, in turn, are taken from the original work by Thoman *et al.* (Ref. 17).

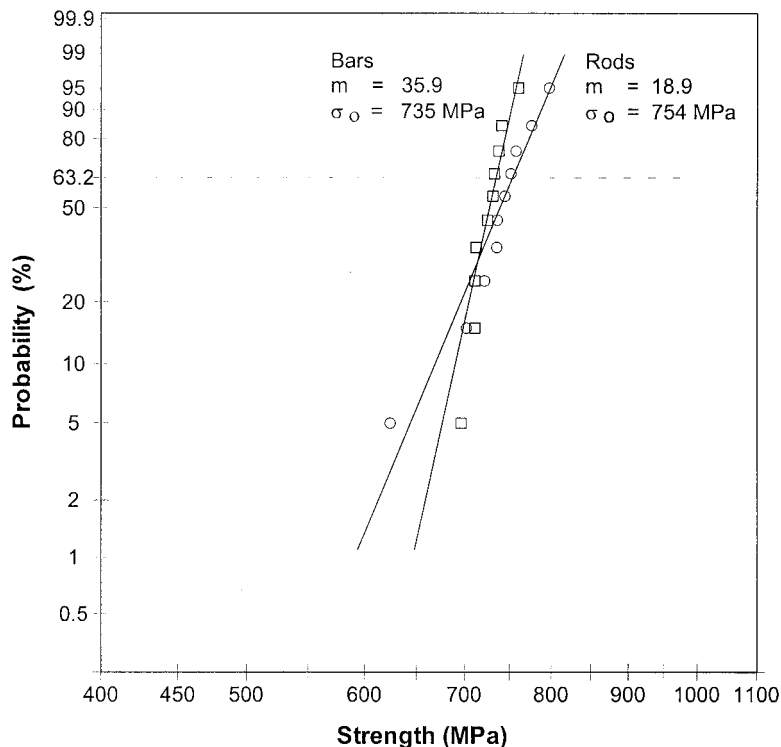


Fig. 4. Rods and bar strengths for SRBSN. The characteristic strength and Weibull modulus is shown for each set.

4.44 mm³, respectively. It is remarkable how inefficient the flexural loaded rods are, in regard to sampling the volume. The effective volume of the rod was only 0.27% of the entire volume (6.00 mm³/2262 mm³), whereas the effective volume of the bars was 0.91% of their entire volume. Equation (1) predicts that the smaller bars should be 1.2% stronger than the rods; however, this observation is opposite of the outcomes shown in Fig. 4.

This example demonstrates a key point about rod flexural-strength data. The physically larger rods had only *slightly larger* Weibull effective volumes than common rectangular specimens. On the other hand, the rods actually had *smaller* effective surfaces. This phenomenon is because rectangular bend bars have a large flat portion on the bottom in the inner gauge section that experiences the full σ_{\max} .

Studies that feature direct comparisons of flexural strengths of rod and bar specimens that have been comparably prepared are uncommon. Newnham¹⁹ tested as-fired reaction-bonded silicon nitride specimens with either 4 mm × 4 mm square or a 4-mm-diameter round cross sections. The strengths differed by only 0%–5%, depending on whether fixtures with rolling or fixed loading pins were used. Test-method errors from frictional constraints in the fixed-pin fixtures interfered with the strength comparisons. Stanley and associates at Nottingham⁸ evaluated identical as-fired reaction-bonded silicon nitride also with 4 mm × 4 mm square and 4-mm-diameter round specimens with four-point 1/4-point flexure with 50-mm spans. The strengths of square specimens and circular specimens were indistinguishable. In a recent design project for ceramic diesel valves, Andrews *et al.*²⁰ compared strengths from rectangular and rod flexure tests to the strengths of valves that had been loaded in direct tension. Weibull size scaling of strength could not account for the observed strength differences, which suggests that different flaws may have been created in the different specimen types.

IV. Conclusions

Weibull effective surface and volume relationships for rods that have been tested in flexure are derived. Flexural loading of rods is inefficient for either volume- or surface-distributed flaws. Strength scaling ratios are independent of whether the flaws are surface- or volume-distributed for rods of the same diameter, irrespective of the rod length.

References

- ¹D. G. S. Davies, "The Statistical Approach to Engineering Design in Ceramics," *Proc. Br. Ceram. Soc.*, **22**, 429–52 (1973).
- ²W. Weibull, "A Statistical Distribution Function of Wide Applicability," *Ingeniörsvetenskapskad. Handl.*, **151**, 1–45 (1939).
- ³A. De S. Jayatilaka and K. Trustrum, "Statistical Approach to Brittle Fracture," *J. Mater. Sci.*, **12**, 1426–30 (1977).
- ⁴R. J. Danzer, "General Strength Distribution Function for Brittle Materials," *J. Eur. Ceram. Soc.*, **10**, 461–92 (1992).
- ⁵G. D. Quinn and R. Morrell, "Design Data for Engineering Ceramics: A Review of the Flexure Test," *J. Am. Ceram. Soc.*, **74** [9] 2037–66 (1991).
- ⁶N. A. Weil and I. M. Daniel, "Analysis of Fracture Probabilities in Nonuniformly Stressed Brittle Materials," *J. Am. Ceram. Soc.*, **47** [6] 268–74 (1964).
- ⁷G. D. Quinn, "Weibull Strength Scaling for Standardized Rectangular Flexural Specimens," *J. Am. Ceram. Soc.*, **86** [3] 508–10 (2003).
- ⁸P. Stanley, H. Fessler, and A. D. Sivill, "The Unit Strength Concept in the Interpretation of Beam Test Results for Brittle Materials," *Proc. Inst. Mech. Eng.*, **190** [49] 585–95 (1976).
- ⁹H. Fessler, A. D. Sivill, and P. Stanley, "Thermomechanical Stress Analysis of Silicon Nitride Components," Defense Research Information Centre Rept. No. DRIC BR 46801, Orpington, Kent, U.K., June 1975.
- ¹⁰B. Roebuck, "Bend Strength Measurements for Hardmetals, International Pre-standardisation Collaborative Activity, Part 2, Analysis of Results," Versailles Advanced Materials and Standards Rept. No. 31, Sept. 1997 (ISSN 1016-2186).
- ¹¹R. Morrell and M. S. Pierce, "A Study of the Room Temperature Strength of a 95% Alumina Ceramics," Sept. 1979 (private communication, R. Morrell to G. Quinn, 2001).
- ¹²G. J. DeSalvo and R. M. Stanchik, "Theory and Application of Weibull Statistics," Westinghouse Astronuclear Laboratory Rept. No. WANL TME-2608, May 1970.
- ¹³P. Kittl and G. Diaz, "Integral Equations in Fracture Statistics of Round Beams of Brittle Materials," *J. Mater. Sci. Lett.*, **3**, 229–31 (1984).
- ¹⁴G. D. Quinn, L. K. Ives, and S. Jahanmir, "On the Nature of Machining Cracks in Ground Ceramics: Part I: SRBSN Strengths and Fractographic Analysis," submitted to *Machin. Sci. Technol.* (2002).
- ¹⁵G. D. Quinn, L. K. Ives, S. Jahanmir, and P. Koshy, "Fractographic Analysis of Machining Cracks in Silicon Nitride Rods and Bars," pp. 343–65 in *Ceramic Transactions, Vol. 122, Fractography of Glasses and Ceramics IV*. Edited by J. Varner and G. Quinn. American Ceramic Society, Westerville, OH, 2001.
- ¹⁶"Standard Practice for Fractography and Characterization of Fracture Origins in Advanced Ceramics," ASTM C 1322-96, *ASTM 2002 Annual Book of Standards*, Vol. 15.01. American Society for Testing and Materials, West Conshohocken, PA, 2002.
- ¹⁷"Standard Practice for Reporting Uniaxial Strength Data and Estimating Weibull Distribution Parameters for Advanced Ceramics," ASTM C 1239-93, *ibid.*
- ¹⁸D. R. Thoman, L. J. Bain, and C. E. Antle, "Inferences on the Parameters of the Weibull Distribution," *Technometrics*, **11** [3] 445–60 (1969).
- ¹⁹R. C. Newnham, "Strength Tests for Brittle Materials," *Proc. Br. Ceram. Soc.*, **25**, 281–93 (1975).
- ²⁰M. J. Andrews, A. A. Wereszczak, and K. Breder, "Predictions of the Inert Strength Distribution of Si₃N₄ Diesel Valves," *Ceram. Eng. Sci. Proc.*, **20** [3] 555–63 (1999). □